10428–10440 *Nucleic Acids Research, 2020, Vol. 48, No. 18* *Published online 22 September 2020*
doi: 10.1093/nar/gkaa771

Influenza A virus co-opts ERI1 exonuclease bound to histone mRNA to promote viral transcription

Marion Declercq[1], Elise Biquand[1], Marwah Karim[1], Natalia Pietrosemoli[2], Yves Jacob[1], Caroline Demeret[1,*,†], Cyril Barbezange[1,*,†] and Sylvie van der Werf[1,*,†]

[1]Unité Génétique Moléculaire des Virus à ARN, UMR3569 CNRS, Université de Paris, Département de Virologie, Institut Pasteur, Paris, France and [2]Bioinformatics and Biostatistics Hub, Department of Computational Biology, Institut Pasteur, USR 3756 CNRS, Paris, France

Received July 31, 2019; Revised August 18, 2020; Editorial Decision August 19, 2020; Accepted September 10, 2020

ABSTRACT

Cellular exonucleases involved in the processes that regulate RNA stability and quality control have been shown to restrict or to promote the multiplication cycle of numerous RNA viruses. Influenza A viruses are major human pathogens that are responsible for seasonal epidemics, but the interplay between viral proteins and cellular exonucleases has never been specifically studied. Here, using a stringent interactomics screening strategy and an siRNA-silencing approach, we identified eight cellular factors among a set of 75 cellular proteins carrying exo(ribo)nuclease activities or involved in RNA decay processes that support influenza A virus multiplication. We show that the exoribonuclease ERI1 interacts with the PB2, PB1 and NP components of the viral ribonucleoproteins and is required for viral mRNA transcription. More specifically, we demonstrate that the protein-protein interaction is RNA dependent and that both the RNA binding and exonuclease activities of ERI1 are required to promote influenza A virus transcription. Finally, we provide evidence that during infection, the SLBP protein and histone mRNAs co-purify with vRNPs alongside ERI1, indicating that ERI1 is most probably recruited when it is present in the histone pre-mRNA processing complex in the nucleus.

INTRODUCTION

RNA decay is a central cellular process that regulates RNA stability and quality, and thereby gene expression (reviewed in (1,2)). Controlling transcript stability is essential to ensure proper cellular physiology and the establishment of adapted responses to viral infection. Growing evidence points to the existence of a large interplay between eukaryotic RNA turnover machineries and viral proteins. On the one hand, viruses evolved mechanisms to evade RNA degradation pathways, and on another hand, they can manipulate these pathways to promote their replication (reviewed in (3–8)).

Many cellular exonucleases involved in RNA decay are known to restrict viral replication. The exonucleases Xrn1 and Xrn2 restrict hepatitis C virus replication in association with the 5′ RNA triphosphatase DUSP11 (9,10). Several RNA viruses are also sensitive to the nonsense-mediated decay pathway because of shared features with aberrant RNAs, such as the presence of multiple ORFs on the same RNA or large 3′ untranslated regions (reviewed in (6)). Some core components of the RNA exosome, a major cellular RNA surveillance machinery, as well as two associated exonucleases, Rrp6 and Dis3, were shown to restrict the replication of vesicular stomatitis virus, Sindbis virus and Rift Valley fever virus (11). Conversely, components of RNA decay machineries were reported to support viral replication. The Sm-like proteins (Lsm1–7) are known for their involvement in mRNA degradation and yet, they are hijacked by several viruses to promote viral RNA translation and replication (12,13). The cytoplasmic 5′-3′ exoribonuclease NbXRN4 was reported to promote the replication of Bamboo Mosaic virus (14). The putative 3′-5′ RNA exonuclease ERI3 associates with DENV-2 ge-

*To whom correspondence should be addressed. Tel: +33 1 45 68 80 00; Email: sylvie.van-der-werf@pasteur.fr
Correspondence may also be addressed to Cyril Barbezange. Email: cyril.barbezange@sciensano.be
Correspondence may also be addressed to Caroline Demeret. Email: caroline.demeret@pasteur.fr
†The authors wish it to be known that, in their opinion, the last three authors should be regarded as Joint Last Authors.
Present addresses:
Elise Biquand, Centre d'Etude des Pathogènes Respiratoires (CEPR), UMR1100, Université de Tours, Tours, France.
Marwah Karim, Department of Medicine and Department of Microbiology and Immunology, Stanford University School of Medicine, Stanford, USA.
Cyril Barbezange, Belgian National Influenza Centre, Viral Diseases Service, Sciensano, Brussels, Belgium.

nomic RNA and is required for viral RNA synthesis (15). Lastly, flaviviruses were shown to exploit the exonuclease Xrn1 to produce non-coding subgenomic RNAs required for pathogenicity (16).

Influenza A viruses (IAV) also rely on cellular proteins to complete their cycle through complex and highly coordinated virus-host interactions (reviewed in (17,18)). IAVs are major pathogens responsible for seasonal epidemics and occasional pandemics (19). Their segmented, negative sense RNA genome is encapsidated with the nucleoprotein (NP) and associated to the heterotrimeric polymerase (FluPol), thus forming the viral ribonucleoproteins (vRNP). In the nucleus of infected cells, the FluPol, composed of PB1, PB2 and PA, conducts the transcription of the genomic viral RNA (vRNA) into viral messenger RNA (mRNA) and the replication of vRNA *via* an intermediate, complementary RNA (cRNA) (reviewed in (20)). Viral mRNA synthesis is primed through short oligonucleotides snatched from capped cellular transcripts by the cap binding domain of PB2 and the endonuclease domain of PA (reviewed in (21)). Polyadenylation occurs through stuttering of the polymerase at an oligoU stretch near the 5′ end of the vRNA. Additional viral proteins that associate to the vRNPs are implicated in the regulation of transcription and replication (NS1, NEP) or mediate nuclear export of neosynthesized viral vRNPs (M1 and NEP) (22–24).

Some exonucleases were reported to restrict or support the replication of influenza A viruses. Interferon-stimulated exonuclease gene 20 protein (ISG20) interacts with influenza virus NP and inhibits viral replication (25). Binding of NS1 to viral dsRNA produced during viral replication counteracts IFN-α/β-induced RNase L activation (26). PA-X endonucleolytic cleavage of host transcripts followed by their degradation by the 5′-3′ exonuclease Xrn1 was shown to promote host shut off (27). Recently, the RNA exosome, known to restrict many RNA viruses, was found to be hijacked by the IAV FluPol to snatch 5′ caps from host non-coding RNAs or mRNAs that would otherwise be targeted to degradation (28).

This led us to systematically screen interactions between IAV viral proteins that constitute or bind to the vRNPs and a selected set of 75 cellular proteins carrying exoribonuclease (Exo) activities or associated with RNA decay (RDec) processes (referred to as the ExoRDec library). Influenza A virus proteins exhibited preferential targeting of RNA degradation pathways and eight targeted cellular factors were identified as contributing to viral multiplication. Among them, ERI1, a 3′-5′ cellular exoribonuclease of the DEDDh family involved in the processing of small RNA, ribosomal RNA and histone mRNA (29–36), was found to interact with several components of the vRNPs and to be required for viral mRNA transcription. We provide evidence that, in infected cells, vRNPs co-opt the histone mRNA trimming complex through binding to exonuclease ERI1 to promote viral transcription.

MATERIALS AND METHODS

Cells, drugs and viruses

HEK-293T and A549 cells were grown in Dulbecco's modified Eagle's medium (DMEM) supplemented with 10% fetal calf serum (FCS). MDCK and MDCK-SIAT cells (37) were grown in Modified Eagle's Medium (MEM) supplemented with 5% FCS. Cycloheximide (CHX, Sigma) was added to the medium (100 μg/ml) at the time of infection. The A/WSN/33(H1N1), A/Paris/650/2004(H1N1), A/Bretagne/7608/2009(H1N1pdm09) and A/Centre/1003/2012(H3N2) viruses were produced by reverse genetics. For the siRNA screen, cells were infected with A549 cell-adapted H1N1pdm09 and H3N2 viruses obtained by reverse genetics as described in (38).

Plasmids

The Gateway entry plasmids containing the ExoRDec ORFs were obtained from the human ORFeome resource. To generate vectors encoding Gluc1-, Gluc2-, GlucFL-, 3XFlag and Strep-fusion proteins, the ORFs were transferred respectively into a Gateway-compatible pGluc-GW, pCIneo3XFlag-GW or pIBA105-GW destination plasmid. All constructs were verified by Sanger sequencing and the sequences were deposited into GenBank under accession numbers MT966965 to MT966999.

Gaussia princeps protein complementation assay (GPCA)

HEK-293T cells were seeded into white 96-well plates at 3 × 10^4 cells/well. After 24h, cells were transfected with linear PEI (polyethylenimine) (Polysciences Inc.) with 200 ng of plasmid expressing a viral protein fused to Gluc1 at its N-terminus (PB1, PB1, PA, NP, NS1, NEP) or at its C-terminus (M1) and 100 ng of a Gluc2-ExoRDec-expressing plasmid. At 24 h post-transfection, cells were washed with 100 μl of phosphate buffered saline and lysed with 40 μl of Renilla lysis buffer (Promega E2820) for 30 min at room temperature. *Gaussia princeps* luciferase enzymatic activity was measured with a Berthold Centro LB960 luminometer by injecting 50 μl of luciferase substrate reagent (Promega E2820) per well and measuring luminescence for 10s. Results were expressed in relative luminescence units.

Normalized luminescence ratio (NLR) retesting

For the NLR method, the Gluc1-viral proteins/Gluc2-ExoRDec pairs were tested in GPCA along with controls consisting of 200 ng of Gluc1-viral proteins plus 100 ng of Gluc2 and 200 ng of Gluc1 plus 100 ng of Gluc2-ExoRDec. The NLR was calculated as the fold change of protein pairs values over the sum of the control values. For a given protein pair A and B, NLR = (Gluc1-A + Gluc2-B)/[(Gluc1-A + Gluc2) + (Gluc1 + Gluc2-B)] (39). NLR validation experiments were conducted three times for each ExoRDec factor. As described in (38), for each viral protein tested, a Random Reference Set of 11 factors was used to calculate a 99.73% confidence interval. The upper limit of the confidence interval was set as the positive threshold.

KEGG pathways enrichment analysis

Functional enrichment analysis was performed using the ClueGO Cytoscape plug-in v2.5.1 (40). The analysis consisted in determining if certain ExoRDec factors showed statistically significant differences regarding the KEGG pathways (41) they were associated to. This enrichment was

calculated for two lists of ExoRDec factors: i) interacting and ii) not interacting with viral proteins, along with their first neighbors in the human proteome retrieved from the APID2net database (42), of 294 and 664 proteins respectively. ClueGO parameters were set as follows: statistical test used = enrichment/depletion (two-sided hypergeometric test), multiple test correction method used = Benjamini–Hochberg, combine clusters with 'or' = true, percentage for a cluster to be significant = 75.0, kappa score threshold = 0.45.

Small interfering RNA assays

siRNAs were purchased from Dharmacon (ON-TARGETplus SMARTpools and Non-Target Control pool). Individual siRNAs targeting ERI1 were purchased from Sigma Aldrich. A549 cells were transfected with 25 nM siRNA with the Interferine transfection reagent (Polyplus). siRNAs targeting FANCG, COPS5 and NUP62 factors, known from the literature to be required for IAV replication, were used as controls (43,44). At 48 h post-transfection, cells were infected with the A/WSN/33(H1N1) at a multiplicity of infection (moi) of 10^{-4} pfu/cell or with A549 cell-adapted A/Bretagne/7608/2009 (H1N1pdm09) and A/Centre/1003/2012(H3N2), or with A/Paris/650/2004(H1N1) (moi 10^{-3} pfu/cell) virus for 24 h. Plaque assays with MDCK-SIAT cells were performed as described in (45). Cell viability was determined using the CellTiter-Glo Luminescent Viability Assay kit according to the manufacter's instructions (Promega). To control the efficiency of siRNAs targeting ExoRDec genes, siRNA-treated A549 cells were transfected with plasmids encoding ExoRDec proteins fused with the full-length *Gaussia* luciferase (pGlucFL-ExoN) using linear PEI (polyethylenimine). The luciferase activity was measured 24h later in cell lysates using the Renilla luciferase assay reagent (Promega) and a Berthold CentroXS luminometer as described before for GPCA.

Antibodies and immunoblots

Protein extracts were prepared in Laemmli buffer. Immunoblot membranes were incubated with primary antibodies directed against ERI1 (MABE894, Merck), A/PR/8/34 virions (46), NS1 (kindly provided by Daniel Marc, INRA-Tours, France), PB2 (GTX125926, GeneTex), NP (HT103, Kerafast), M1 (GA2B, Pierce), M2 (MA1-082, ThermoFisher Scientific), NA (GTX125974, GeneTex), GAPDH (Pierce), α-Tubulin (T6199, Sigma), *Gaussia* luciferase (E8023, New England Biolabs), and revealed with secondary antibodies (GE Healthcare) or peroxidase-conjugated Strep-Tactin (IBA), with the ECL 2 substrate (Pierce). The chemiluminescence signals were acquired using a G-Box and the GeneSnap software (SynGene).

Overexpression experiments

HEK 293T cells were seeded in 24-well plates at 5×10^5 cells per well and transfected with 60 ng of Strep-ERI1 plasmids with linear PEI (polyethylenimine). At 24 h post-transfection, cells were infected with A/WSN/33(H1N1) at an moi of 5 pfu/cell. At 3 hpi total RNA was extracted using the RNeasy mini kit (Qiagen) and viral RNAs were quantified as described below.

RT-qPCR assays

RNAs were extracted using the RNeasy mini kit (Qiagen) from A/WSN/33(H1N1) infected A549 cells. Strand-specific RT-qPCR for NP and NA vRNAs and mRNAs was performed as described in (47). Briefly, cDNAs complementary of NP and NA vRNAs and mRNAs were synthesized using tagged primers in order to add a strand specific tag unrelated to influenza virus at the 5′ end. Tagged cDNAs were then used as a template for the qPCR reaction using a tag specific primer and a segment specific primer. For HIST1H2AB mRNA amplification reverse transcription was carried out using random hexamer and SuperScript II (Thermo Fisher Scientific) following the manufacturer's instructions. All qPCRs were performed using SYBR green reagent (Agilent Technologies) on a Light Cycler 480 (Roche) using primers as described in (47) to specifically detect NP and NA mRNAs and vRNAs, or HIST1H2AB F (5′-cacacgccccaagagtttat-3′) and HIST1H2AB R (5′-ctccgc aaaggcaactactc-3′) primers to detect HIST1H2AB mRNA (48).

Strep-tag and PB2 pull-down

HEK-293T cells were transfected with Strep-ERI1 or Strep-empty expressing plasmids using linear PEI (polyethylenimine) and infected with A/WSN/33(H1N1) at an moi of 5 pfu/cell. Infected HEK-293T cells were resuspended in lysis buffer (20 mM MOPS–KOH pH 7.4, 120 mM KCl, 0.5% Igepal, 1× protease inhibitor Cocktail (Roche) supplemented with 200 U/ml RNasin (Promega) or 100 μg/ml RNase (Thermo Fisher Scientific)). For Strep-tag purification, clarified lysates were incubated with Strep-Tactin beads (Strep-Tactin Sepharose High Performance, GE Healthcare) for 1 h at 4°C. Beads were washed three times in lysis buffer. Protein complexes were eluted from Strep-Tactin beads with desthiobiotin (IBA). For PB2 purification, clarified lysates were cleared for 1 h at 4°C with dynabeads protein A (Invitrogen) to remove aspecific binding and then incubated with anti PB2 antibody (GTX125926, Genetex) overnight at 4°C. Protein complexes were allowed to bind to protein A dynabeads for 1 h at 4°C. Beads were washed three times in lysis buffer. Pulled samples were diluted in Laemmli sample buffer and analyzed by western blot. For histone mRNA co-purification, PB2 pull down was performed as previously described. Beads were diluted in RLT buffer (RNeasy mini kit, QIAGEN) and RNA purification was performed according to the manufacturer's instructions. Reverse transcription and subsequent qPCR for histone mRNA detection was performed as described above.

RESULTS

Gaussia princeps protein complementation assay (GPCA) screening of the ExoRDec library

The 75 cellular proteins composing the ExoRDec library, selected using GO terms associated to exonucleases and RNA decay (Supplementary Tables S1, S2),

were systematically screened for interaction with viral proteins (PB2, PB1, PA, NP, M1, NS1 and NEP) from IAV strains A/Paris/650/2004(H1N1) (sH1N1) and A/Bretagne/7608/2009(H1N1pdm09) (pH1N1) by a split *Gaussia* luciferase assay as previously described in (38) (Supplementary Figure S1). This initial screening identified two to nine cellular proteins as putative interacting partners for each viral protein. These interactions were retested using the NLR (Normalized Luminescence Ratio) method as described in (39) to take into account the background noise of interaction and the expression level of each tested partner, thus discriminating between true interacting partners and false positives. Nineteen ExoRDec proteins were validated as interactors of at least one viral protein (Supplementary Table S3 and Figure 1A). The interaction profiles between sH1N1 and pH1N1 were almost identical (Supplementary Table S3), and several ExoRDec factors were found to interact with more than one viral protein (Figure 1A); ADARB1, ERI1, EXOSC6 as well as ADAR and HMGA2 were the most connected, with interactions validated to four and three viral proteins, respectively. The direct interactors (first neighbors) of each factor of the ExoRDec library were retrieved from the human proteome interaction network. Cellular process enrichment analysis of all these cellular proteins revealed a specific enrichment in RNA degradation processes only for the viral-protein-interacting ExoRDec factors and their first neighbors (Figure 1B).

Small interfering RNA screening of ExoRDec interactors identifies ERI1 as a factor required for IAV replication

The role of the 19 validated ExoRDec factors on the viral life cycle was further investigated using small interfering RNA (siRNA)-mediated silencing. Upon siRNA knock down of these 19 factors, A549 cell viability remained above 80% compared to the non-target treated cells, except for INPP5K (Supplementary Figure S2A), and limited knock down efficiency (<50%) was observed for seven factors (Supplementary Figure S2B). Knock down of eight of the ExoRDec proteins was found to significantly impair IAV multiplication (Supplementary Figure S2C). We chose to focus on ERI1, a 3′-5′ cellular exoribonuclease involved in multiple cellular RNA maturation and degradation processes, for which a redundant targeting by viral proteins was found by GPCA (Figure 1A). Silencing of ERI1 by two individual siRNAs confirmed the results of the siRNA screen, and ERI1 was found to impair the viral life cycle of four different IAV strains (Figure 2A and Supplementary Figure S3A). The effects are lasting over time and the production of infectious viral particles in ERI1 knock down cells remained lower than in non-target treated cells at several time points post-infection (Figure 2B).

ERI1 interacts with IAV vRNP components

ERI1 was identified by GPCA as an interactor of the PB2, PB1, NP and M1 viral proteins. The lower NLR values obtained with PB1 and especially M1 indicate a weaker association of ERI1 with these viral proteins (Figure 2C), suggesting that, within the vRNPs, PB2 and NP are the main targets of ERI1. Co-immunoprecipitation experiments using transient transfection expression in HEK-293T cells further confirmed the specific interaction of ERI1 with PB2 and NP, and to lesser extend with PB1, while no significant interaction was detected for M1, corroborating the GPCA results (Figure 2D). In addition, the binding of PB2 and of NP to ERI1 was still detected under RNase treatment, both in GPCA and co-immunoprecipitation assays, while the interaction with PB1 was lost in co-immunoprecipitation (Supplementary Figure S3C, D). Overall, these data demonstrate a direct, RNA-independent interaction of ERI1 with the viral PB2 and NP proteins. Interestingly, when PB2, PB1 and PA were expressed along with Strep-ERI1 or Strep-mCherry, all three viral proteins were retrieved upon Strep-ERI1 purification (Figure 2E), suggesting that ERI1 might interact with the tripartite polymerase complex.

Viral transcription is impaired in ERI1 silenced cells leading to a delay in viral protein accumulation

The role of ERI1 on the virus life cycle was further studied in A549 cells silenced by ERI1 siRNA in comparison to non-target siRNA treated cells as control. During single cycle infection in ERI1 silenced A549 cells compared to control, the accumulation of the viral proteins PB2, NP and NS1 was reduced at 3hpi. Such decrease was less obvious at 6 hpi, at which point accumulation of the late viral proteins M1, M2 and NA was slightly reduced (Figure 3A). The effects of ERI1 depletion were thus primarily detected during the initial steps of viral protein accumulation, suggesting an involvement of ERI1 from the early stages of the viral life cycle, possibly during transcription. Indeed, viral mRNA production was reduced in ERI1 silenced A549 cells compared to control as soon as 3hpi, and more obviously at 6hpi (Figure 3B). Likewise, a decrease in vRNA production was also apparent at 6hpi in ERI1 silenced cells. This might be a consequence of the decreased production of viral proteins due to impaired viral transcription (Figure 3A, B), since the synthesis of new genomic vRNA requires the accumulation of neo-synthesized viral replication proteins. Conversely, overexpression of ERI1 led to an increase in viral transcription as assessed by mRNA/vRNA ratios (Figure 3C). Last, these ratios were also reduced in ERI1 silenced cells (compared to cells treated with control siRNA) under cycloheximide (CHX) treatment that is known to block *de novo* translation (Figure 3D, E). Altogether, these results suggest a role of ERI1 in viral transcription, including in the initial synthesis of mRNA from the incoming vRNPs (viral primary transcription).

ERI1 RNA binding and exonuclease activities are required to promote viral transcription

ERI1 can be schematically divided into two domains, the N-terminal domain containing a nucleic-acid binding 'SAF-box, Acinus and PIAS' (SAP) sub domain and the C-terminal domain containing the exonuclease activity, connected by a small inter-domain spacer (30) (Figure 4A). Overexpression experiments with ERI1 wild-type (wt) or with mutants for RNA binding (R105A, ΔSAP) or DEDDh exonuclease activity (D134A+E136A, i.e. no-DE)

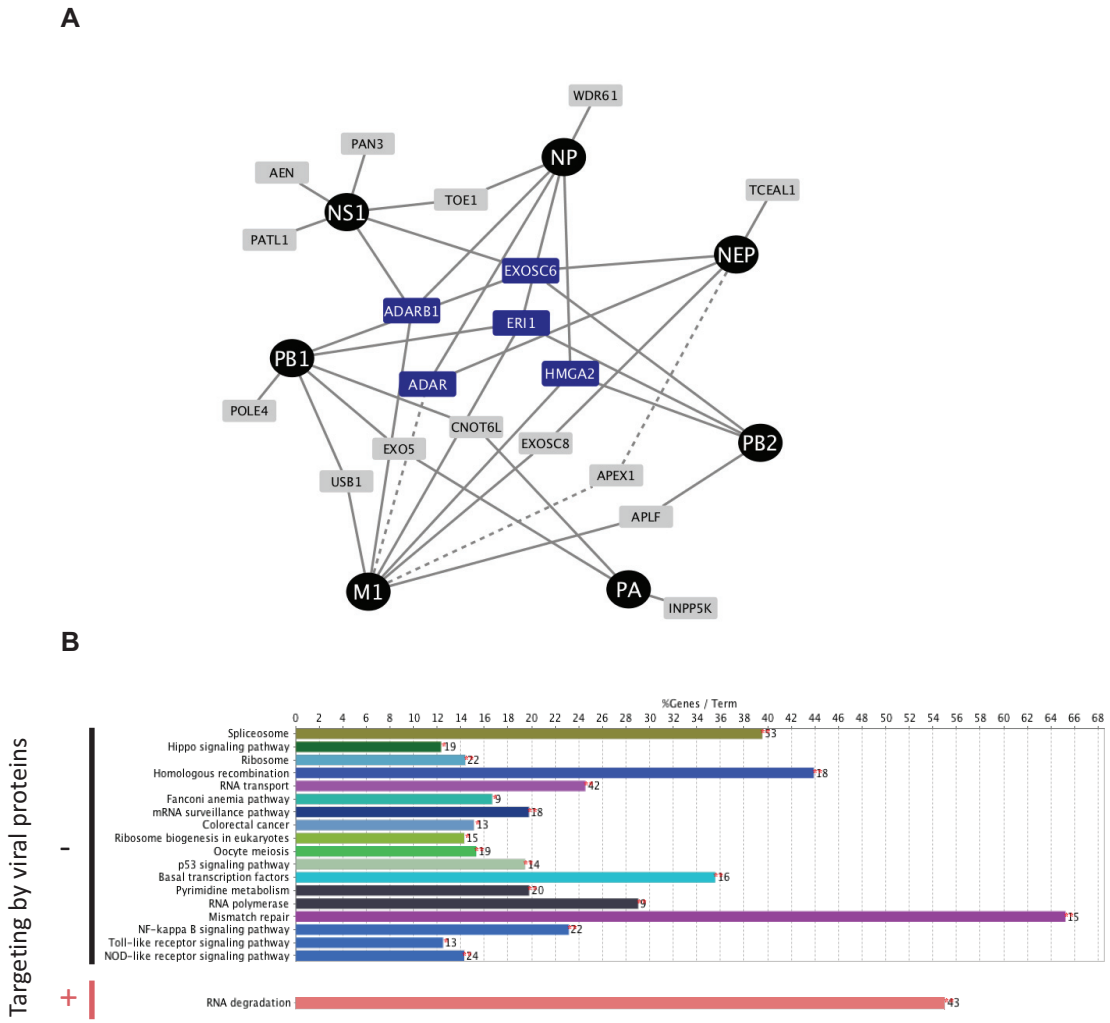

Figure 1. Systematic screening of the ExoRDec library. (**A**) Interaction network of validated PPIs after NLR retesting. Viral proteins are indicated in black circles, factors of the ExoRDec library in grey boxes. Redundant targeting (i.e. cellular protein targeted by three or more viral proteins) is depicted with blue boxes. Edges that were only found with viral protein of pH1N1 are indicated with dashed lines. (**B**) KEGG pathways enrichment analysis. The ExoRDec library and associated proteome was divided in two clusters, i.e. non-targeted (−) and targeted (+) by viral proteins. Each bar corresponds to a KEGG pathway found to be statistically significant (P-value < 0.05) in each cluster. The length of the bar represents the proportion of genes belonging to the pathway that are present in the cluster with respect to the whole pathway. The number associated to each bar corresponds to the total number of genes present in the cluster for the given pathway. Enrichment analysis was carried out using the ClueGO plug-in of Cytoscape as described in the methods section.

were used to decipher which of these activities contributes to the role of ERI1 in IAV multiplication. While overexpression of ERI1 wt led to a two-fold increase in viral transcription, overexpression of R105A, ΔSAP or no-DE mutants was not associated with such increase in viral transcription, even though they accumulated at the same levels as ERI1 wt (Figure 4B, C). Overexpression of the no-DE mutant even led to a slight decrease in viral transcription. Given that ERI1 no-DE mutant retained the ability to interact with viral proteins (Supplementary Figure S4A, B) while losing its exonuclease activity, such decrease in viral transcription could be the consequence of a dominant negative effect due to the capture of the viral proteins by a catalytically inactive form of ERI1. In all, both RNA binding and exonuclease activities of ERI1 appear to be required for its role in IAV multiplication.

Association of IAV vRNPs to ERI1 during infection is RNA dependent

In IAV infected cells, purification of endogenous ERI1 specifically co-immunoprecipitated PB2 and NP viral proteins (Figure 4D), confirming in an infectious context the interaction detected by GPCA and transient expression experiments (Figure 2C–E). Conversely, PB2 immunoprecipitation co-purified Strep-ERI1 from the lysates of cells transfected with Strep-ERI1 and infected with IAV (Figure 4E), while Strep-ERI1 purification allowed to retrieve the tripartite polymerase complex (Figure 4F).

Since ERI1 RNA binding activity was found to be required for viral transcription (Figure 3B–D), we assessed the involvement of RNA in ERI1 interaction with the vRNPs during infection, using RNase treatment. Unex-

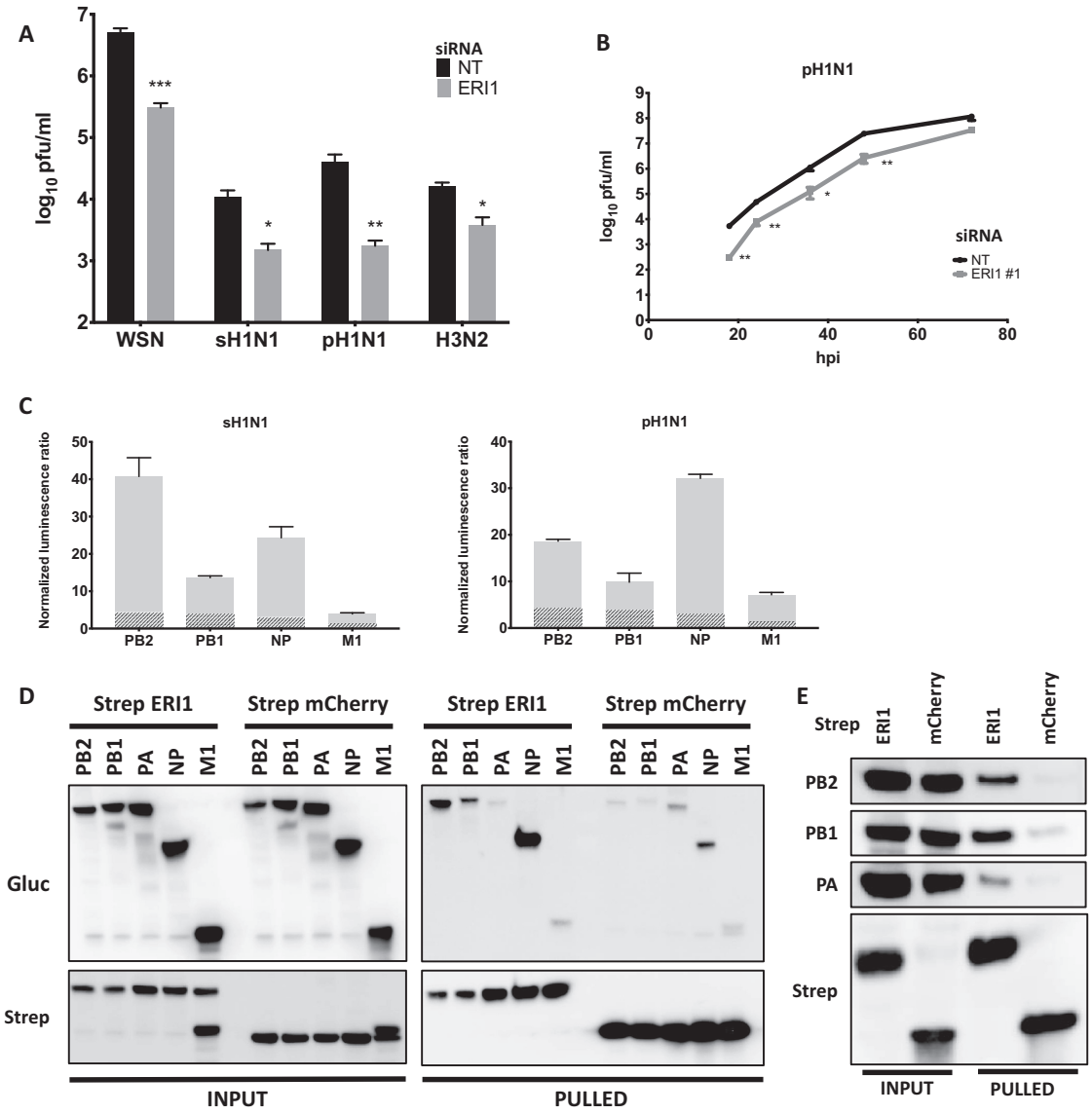

Figure 2. IAV multiplication is impaired in ERI1-depleted cells and ERI1 interacts with viral proteins. (A, B) A549 cells were treated with control (black) or single ERI1 siRNA (gray, ERI1#1) and infected with the following viruses at the indicated moi in pfu/cell: A/WSN/33(H1N1) (WSN, moi 10^{-4}); A/Paris/650/2004(H1N1) (sH1N1, moi 10^{-3}); A/Bretagne/7608/2009(H1N1pdm09) (pH1N1, moi 10^{-4}), A/Centre/1003/2012(H3N2) (H3N2, moi 10^{-3}). At 24 hpi (**A**), or at several time points post-infection (18, 24, 36, 48, 72 hpi) **(B)**, viral titers were determined by plaque assay on MDCK-SIAT cells. The results are expressed as the mean ± SEM of triplicates and the significance was tested with a multiple t test, using the Holm-Sidak method, in GraphPad Prism software ($*P < 0.05$, $**P < 0.01$, $***P < 0.001$). (**C**) Interaction of ERI1 with sH1N1 and pH1N1 viral proteins was tested by applying the NLR (normalized luminescence ratio) method that takes into account the background noise of interaction of the Gluc1 or Gluc2 fusion partners. Positive threshold values, calculated as in (38), are represented by hatched bars. The results are expressed as the mean ± SEM of triplicates. (**D**) HEK-293T cells were co-transfected with Strep-ERI1 or Strep-mCherry (as a control), and Gluc1-PB2-WSN, -PB1-WSN, -PA-WSN, -NP-WSN or –M1-WSN. At 24 hpt, Strep tagged proteins were purified with sepharose Strep-Tactin beads. PA, found as a non-interacting partner of ERI1 in our GPCA screen was used as a control of non-specific interaction. Strep-tagged eluates were analyzed by immunoblot to detect Strep and Gluc1 tagged proteins. Results representative of three independent experiments are shown. (**E**) HEK-293T cells were co-transfected with Strep-ERI1 or Strep-mCherry (as a control) along with untagged PB2, PB1 and PA. At 24 hpt, Strep tagged proteins were purified with sepharose Strep-Tactin beads. Strep-tagged eluates were analyzed by immunoblot to detect Strep and the viral proteins. Results representative of three independent experiments are shown.

pectedly, when RNase was used, viral PB2 and NP proteins were no longer co-purified along with Strep-ERI1, while without RNase the co-immunoprecipitation of PB2 and NP viral proteins was possible (Figure 4G). These results indicate that the interaction of ERI1 with the vRNPs is RNA-dependent in an infectious context, although a direct, RNA-independent interaction of ERI1 with PB2 and NP was detected in co-transfected cells (Supplementary Figure S3C, D). Quantification of the viral NP mRNA and vRNA co-purified with Strep-ERI1 from infected cell lysates showed that a significantly higher proportion of mRNA was co-purified as compared to vRNA (Figure 4H,

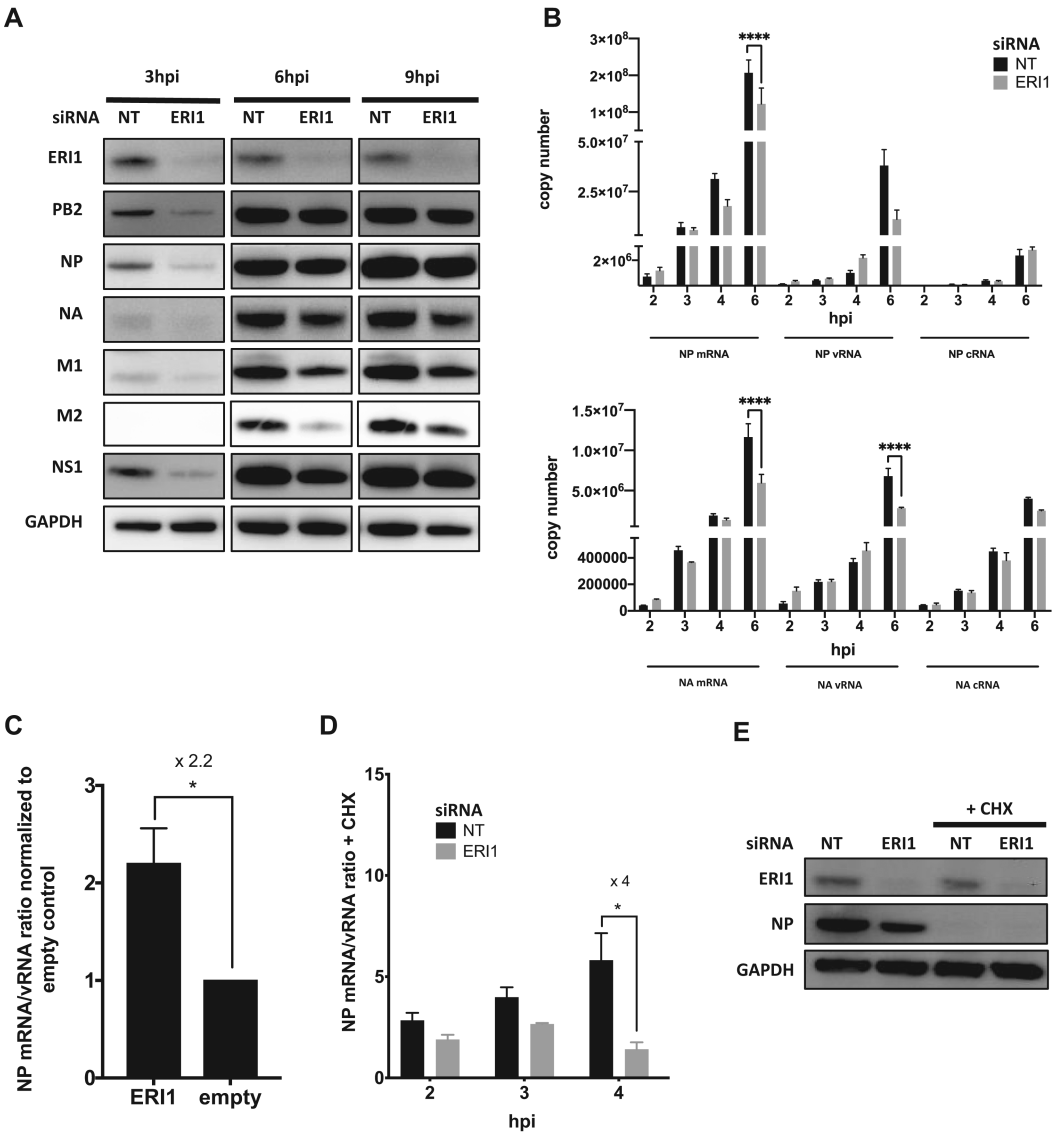

Figure 3. ERI1 silencing alters viral life cycle. (**A**) A549 cells were treated with non-targeting (NT) or ERI1 siRNAs and infected 48hpt with WSN at an moi of 3 pfu/cell. Total cell extracts were prepared at the indicated times post-infection and analyzed by immunoblot using antibodies directed against the indicated proteins. Results representative of three independent experiments are shown. (**B**, **D**, **E**) A549 cells treated with non-targeting (NT, black bars) or ERI1 (gray bars) siRNAs were infected with WSN at an moi of 3 pfu/cell in the absence (B) or presence (D, E) of cycloheximide (CHX) (100μg/ml) that blocks translation. Total RNAs were extracted at the indicated time points post infection and the levels of NP or NA mRNAs, vRNAs and cRNAs were determined by strand specific RT-qPCRs. The results are expressed as the mean ± SEM determined in three independent experiments. The significance was tested by two-way ANOVA with Sidak's multiple correction test in GraphPad Prism Software (****$P < 0.0001$; *$P < 0.05$). (**C**) HEK-293T cells were transfected with Strep-ERI1 or Strep-empty (as a control) and infected with WSN at an moi of 3 pfu/cell. At 3 hpi total RNAs were extracted and the levels of NP mRNAs and vRNAs were determined by strand specific RT-qPCRs. The results are expressed as the mean ratios of mRNA/vRNA ± SEM normalized to empty control, determined in three independent experiments. The significance was tested with an unpaired t-test using GraphPad Prism Software (*$P < 0.05$). (**E**) Total extracts from infected cells treated with non-targeting (NT) or ERI1 siRNAs, and treated with CHX or not, were prepared at 6hpi and analyzed by immunoblot using antibodies directed against the indicated proteins. No viral protein was detectable at 6hpi upon CHX treatment demonstrating that CHX effectively blocked *de novo* translation.

I). In a non-infectious context, we found that viral RNAs, like histone mRNAs, were more co-purified with Strep-ERI1 than with Strep-mCherry, showing that ERI1 is able to bind to viral RNAs (Supplementary Figure S4C). Our data are thus suggesting that ERI1 could be recruited to viral mRNA, possibly through both interactions with NP and PB2 of the vRNPs and direct binding to RNA, in line with a potential role of ERI1 in viral transcription.

vRNPs associate with the SLBP–ERI1–histone mRNA complex

ERI1 nuclear functions comprise histone mRNA maturation. ERI1 participates in the histone pre-mRNA processing complex and binds to the stem loop structure in the 3′UTR of histone pre-mRNA, forming a ternary complex along with the stem loop binding protein (SLBP) (29,30,35,49). The ΔSAP and R105A mutants of ERI1 were

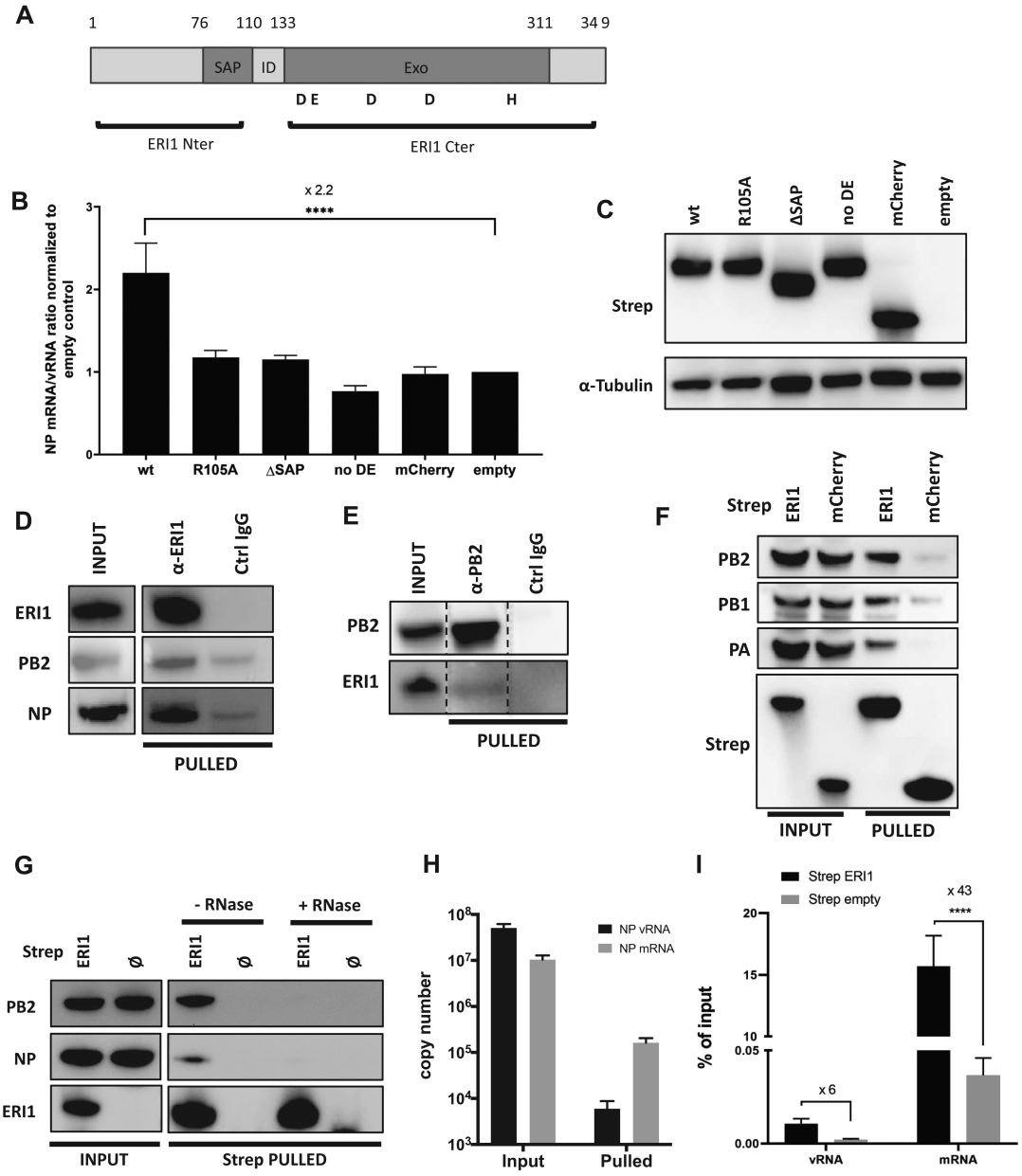

Figure 4. RNA binding and exonuclease activities of ERI1 are both required for IAV cycle. (**A**) Schematic organization of ERI1. The N-terminal part contains the 'SAF-box, Acinus and PIAS' (SAP) domain while the C-terminal part carries the exonuclease activity. (B, C) HEK-293T cells were transfected with Strep-ERI1, Strep-ERI1 mutants (R105A, ΔSAP, D134A+E136A, i.e. 'no DE') or Strep-mCherry (as a control) and infected with WSN at an moi of 3 pfu/cell. At 3hpi total RNAs were extracted and the levels of NP mRNAs and vRNAs were determined by strand specific RT-qPCRs **(B)**, or analyzed by immunoblot to assess protein expression levels (**C**). The results are expressed as the mean ratios of mRNA/vRNA ± SEM normalized to empty control, in three independent experiments. The significance was tested by one-way ANOVA with Holm-Sidak's multiple comparisons test using GraphPad Prism Software ****$P < 0.0001$). (D, E) HEK-293T cells were infected with WSN at an moi of 3 pfu/cell. At 3 hpi, ERI1 protein (**D**) or at 6 hpi, PB2 protein (**E**) was purified using anti-ERI1 antibodies (α-ERI1) (D) or anti-PB2 antibodies (α-PB2) (E) or control immunoglobulins (Ctrl IgG). Inputs and α-ERI1, α-PB2 and Ctrl IgG eluates were analyzed by immunoblot to detect ERI1, PB2 and/or NP. Results representative of two (D) and three (E) independent experiments are shown. (**F**) HEK-293T cells were transfected with Strep-ERI1 or Step-mCherry and infected 24hpt with WSN at an moi of 3 pfu/cell. At 6hpi, Strep-tagged proteins were purified with sepharose Strep-Tactin beads. Inputs and strep eluates were analyzed by immunoblot to detect PB2, PB1, PA and Strep. Results representative of three independent experiments are shown. (**G**) HEK-293T cells were transfected with Strep-ERI1 or Strep-empty and infected with WSN (3 pfu/cell). At 6hpi, Strep-tagged proteins were purified with sepharose Strep-Tactin beads. Complexes bound to the beads were incubated with RNase A (+ RNase) or Rnasin (– RNase) for 1 h. Inputs and Strep-tagged eluates were analyzed by immunoblot to detect ERI1, PB2 and NP. Results representative of three independent experiments are shown. (**H**) The levels of NP vRNAs (black bars) and mRNAs (grey bars) co-purified with Strep-ERI1 as described in (B) are expressed as the mean ± SEM of three independent experiments. The background level of detection in Strep-empty eluates was 9.9×10^2 and 6×10^3 copies for NP vRNAs and NP mRNAs, respectively. (**I**) Viral RNAs co-purified with Strep-ERI1 and Strep-empty (as a control) were expressed as a ratio of the viral RNA quantified in the input. Significance was tested by two-way ANOVA with Sidak's multiple comparisons test using GraphPad Prism Software ****$P < 0.0001$).

previously reported to be impaired for histone mRNA binding and maturation in the nucleus (30,35). Although the ΔSAP lacks almost a whole protein domain, it was shown to be properly folded and functioning (30). In the lysates of IAV infected cells, the proportions of histone mRNA (Figure 5A) and viral NP mRNA (Figure 5B) that were co-purified by the mutants as compared to ERI1 wt were similarly reduced. In addition, the ΔSAP mutant that showed the strongest reduction in interaction with viral proteins in GPCA (Supplementary Figure S4A) was unable to co-immunoprecipitate PB2 and NP viral proteins (Figure 5C), suggesting that the interaction domain of ERI1 with the vRNP could lie in the SAP domain. In infected cell lysates, PB2 purification was found to co-immunoprecipitate both ERI1 and SLBP (Figure 5D). As for the co-purification of ERI1, the co-purification of SLBP with PB2 and NP was sensitive to RNase treatment (Figures 4G and 5E). Furthermore, the PB2 eluates were found to be specifically enriched in several histone mRNAs compared to control eluates (Figure 5F). Histone mRNA co-purification with PB2 was also greatly reduced in ERI1 silenced cells compared to non-target siRNA treated cells (Figure 5G). Taken together, these results support the conclusion that the form of ERI1 that is recruited to vRNPs during IAV infection is bound to histone mRNA and associated with SLBP, as part of the histone pre-mRNA processing complex.

DISCUSSION

A growing body of evidence points to an intricate functional interplay between IAV infection and the cellular RNA decay machineries (25–28,50,51). Our systematic screening strategy further highlights a specific targeting of RNA degradation pathways shared by different H1N1 IAV strains. Furthermore, the detection of an effect on the viral life cycle for eight of 19 interactors identified among the 75 tested from the original ExoRDec library, underscores the performance of the stringent protein-protein interaction screen applied here for the identification of functionally relevant factors. Some of the identified factors have been previously reported to be essential for IAV replication, such as the Double-stranded RNA-specific adenosine deaminase ADAR and the U6 snRNA phosphodiesterase USB1 (52,53), or to be important for the replication of other RNA viruses, such as the Apoptosis-Enhancing Nuclease AEN and the DNA-(apurinic or apyrimidinic site) lyase APEX1 (54–56). Interestingly, redundant targeting was observed in most instances, with factors targeted by three (ADAR, HMGA2) or even four (ADARB1, EXOSC6, ERI1) viral proteins. This redundant targeting may reflect the importance for the virus to target those specific pathways. Remarkably, our study identifies the exosome subunit EXOSC6, found by others to interact with PA, as an interactor of PB2, PB1, NS1 and NEP (28). Such broad targeting of the RNA exosome by viral proteins further highlights its crucial requirement in the IAV life cycle. A more extensive comparative screening with proteins from a wider range of IAV strains will however be required to further generalize these observations. It is interesting to note that the viral protein PA-X was not included in our initial screening of the ExoRDec library because of technical constraints related to the PCA design. As PA-X is known to be tightly associated to RNA decay (57), its screening against the ExoRDec library could also be of great interest.

In the present study, we focused on ERI1 found in our screen as an interactor of PB2, PB1, NP and, to a lesser extent, of M1 proteins of IAV, although subsequent experiments showed that the interaction with PB1 and M1 was probably indirect and mediated by RNA. ERI1 belongs to the DEDDh exoribonuclease family. Some exonucleases in this family have already been reported to be essential for the multiplication of different RNA viruses. For instance, coronavirus nsp14 protein was shown to carry an exoribonuclease activity required to maintain viral replication fidelity, while Lassa fever virus nucleoprotein possesses a DEDDh exonuclease activity essential to suppress host innate immune system activation (58,59). An ERI1 homologue, the putative 3′-5′ RNA exonuclease ERI3, is critical for DENV-2 RNA synthesis and viral particle production, and was found to associate with DENV-2 RNA (15).

In the cell, ERI1 has multiple roles both in the cytoplasm and in the nucleus. In the latter, ERI1 mostly plays a role in histone mRNA maturation, while in the cytoplasm, it is involved in histone mRNA decay, 5.8S rRNA maturation and miRNA homeostasis (29–36). A common feature of all these processes is the prime role of ERI1 in RNA 3′ end trimming. Trimming of histone pre-mRNA by ERI1 requires the recognition of the 3′ stem loop upstream of the processing site. However, ERI1 trimming of other RNA species does not seem to require a specific RNA sequence nor structure aside from the existence of a 3′ ssRNA overhang. Various RNA species can thus be potential substrates for ERI1, but whether these include viral mRNAs is not known. Our data uncovered a role of ERI1 in promoting viral transcription of influenza A viruses, mostly evident during the early stages of the viral life cycle, for which both ERI1 activities - RNA binding and 3′-5′ exoribonuclease activities - were shown to be required. The RNA binding activity requirement could at least be explained by the recruitment of ERI1 when it is stably bound to histone pre-mRNAs in association with SLBP, as supported by our results showing an RNA dependency in an infectious context. Since ERI1 seems also able to directly interact with IAV viral RNA, one could envision that ERI1, recruited as part of the histone processing complex, could then directly interact with the viral proteins of the vRNPs in order to be loaded onto viral RNAs. The role of the exonuclease domain is also not clear at this stage. Interestingly, the exonuclease domain of ERI3 was not shown to be required for its role in promoting Dengue virus 2 mRNA synthesis (15), suggesting that the mechanisms involved in promoting viral transcription, which are also still unknown for Dengue virus, might differ. We observed a clear enrichment in viral mRNAs co-purified with ERI1. Since ERI1 is known to play a role in the maturation of cellular RNAs, one could envisage that ERI1 contributes to the maturation of IAV mRNAs during synthesis, which is necessary for their efficient translation. RNA-seq methodology might be an interesting tool to test this hypothesis.

The differences observed in viral transcription levels between non-target and ERI1 silenced cells, with consequences at the protein level, are unlikely to be linked to a

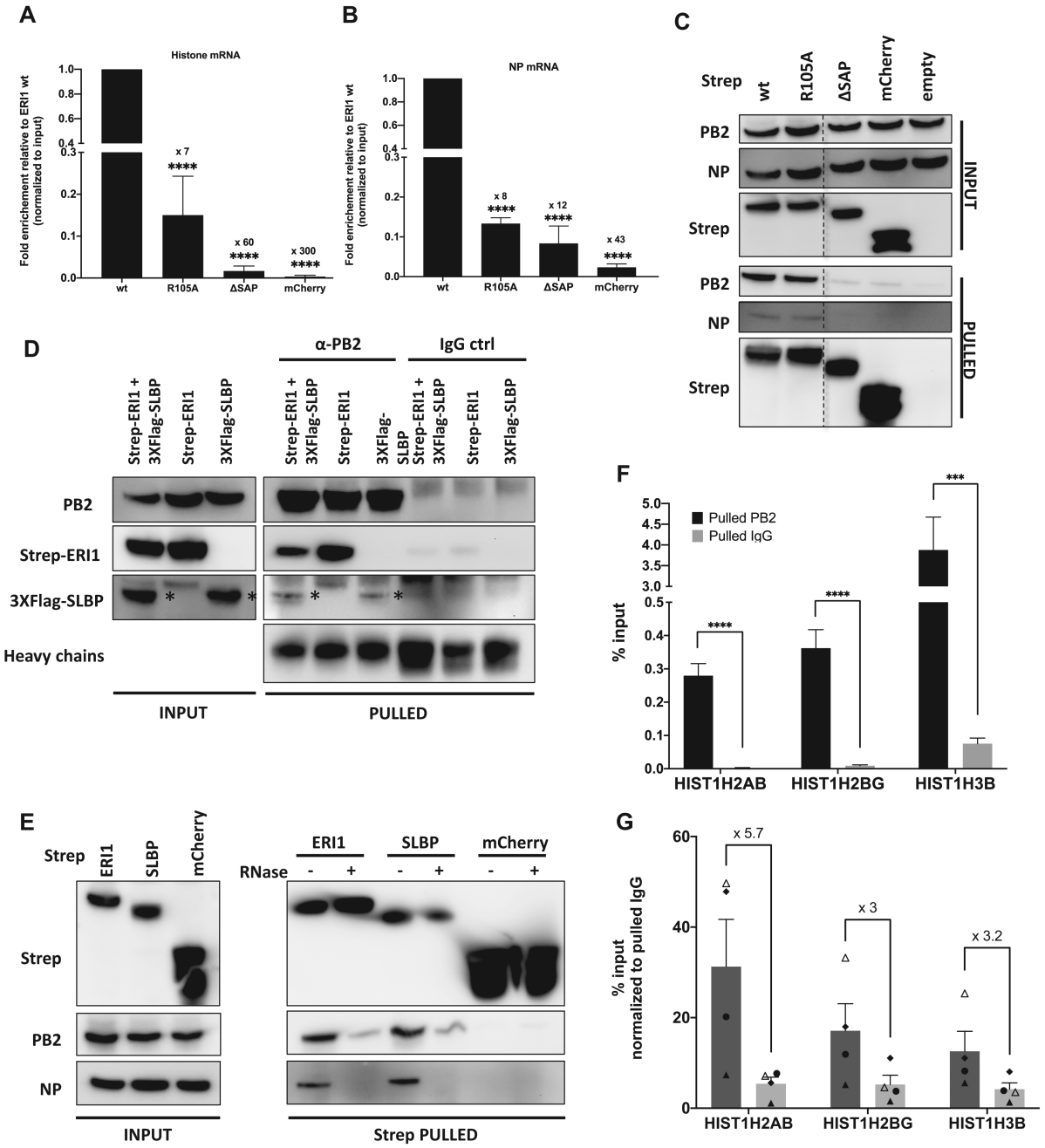

Figure 5. ERI1 is co-purified with histone mRNA and SLBP in infected cells. (A–C) HEK-293T cells were transfected with Strep-ERI1 wild-type (wt), Strep-ERI1 R105A mutant, Strep-ERI1 ΔSAP mutant or with Strep-mCherry or Strep-empty (as a control), and infected with WSN (3pfu/cell). At 6hpi, Strep-tagged proteins were purified with sepharose Strep-Tactin beads. The levels of HIST1H2AB mRNA (**A**) and NP mRNAs (**B**) co-purified with Strep-pulled proteins are expressed as the mean ± SEM of three independent experiments. Statistical significance was assessed by one-way ANOVA test with Dunnett's multiple comparison test (**** $P < 0.0001$). (**C**) Inputs and Strep-pulled eluates were analyzed by immunoblot with the indicated antibodies. (**D**) HEK-293T cells were co-transfected with Strep-ERI1 and 3XFlag-SLBP, or transfected with either Strep-ERI1 or 3XFlag-SLBP, and infected with WSN (moi = 3 pfu/cell). At 6 hpi, PB2 proteins were purified using anti PB2 antibodies (or control immunoglobulins IgG ctrl). Inputs and eluates were analyzed by immunoblot using Strep-Tactin or antibodies directed against 3X-Flag or PB2 to respectively detect Strep-ERI1, 3XFlag-SLBP and PB2. (**E**) HEK-293T cells were transfected with Strep-ERI1, Strep-SLBP or Strep-mCherry and infected with WSN (moi = 3pfu/cell). At 6hpi, Strep tagged proteins were purified with sepharose Strep-Tactin beads. Complexes bound to the beads were incubated with RNase A (+) or Rnasin (−) for 1h. Inputs and eluates were analyzed by immunoblot to detect Strep, PB2 and NP. Results representative of three independent experiments are shown. (**F**) HEK-293T cells were infected with WSN at an moi of 3 pfu/cell. At 6hpi, PB2 proteins were purified using anti-PB2 antibodies. Levels of HIST1H2AB, HIST1H2BG and HIST1H3B mRNA co-purified with PB2 (black) or with control IgG (gray) were quantified using RT-qPCRs. The results are expressed as the mean ± SEM of triplicates and the significance was tested with a multiple t test, using the Holm-Sidak method, in GraphPad Prism software (*** $P < 0.001$, **** $P < 0.0001$). (**G**) HEK-293T cells were treated with NT (dark grey) or ERI1 (light gray) siRNAs. At 48hpt, cells were infected with WSN (moi = 3 pfu/cell). At 6hpi, PB2 proteins were purified using anti-PB2 antibodies. Levels of HIST1H2AB, HIST1H2BG and HIST1H3B mRNA co-purified with PB2 in NT and ERI1 siRNA treated cells were quantified using RT-qPCRs. The results are expressed as the mean ± SEM of triplicates.

role of ERI1 in viral mRNA splicing or export from the nucleus. Indeed, the effect of ERI1 silencing was observed at similar levels for the products of unspliced viral transcripts, such as NP, PB2, NS1 and later NA and M1, and for the M2 protein translated from an M1 spliced transcript. Our data are more in favor of a role of ERI1 in viral mRNA maturation and quality control, whose defect in the very early steps of infection would reduce the efficiency of early protein synthesis following primary transcription. A decreased production of the viral proteins involved in transcription/replication of the viral genome could then induce a reduction of the secondary produced viral transcripts at later times post infection, consistent with what we observed at the protein level.

ERI1 could have indirect roles too. For example, like the exonuclease activity of Lassa virus NP which was shown to inhibit innate immunity (59), ERI1 during IAV infection could be hijacked to modulate the innate immunity in order to promote viral transcription. On the other hand, ERI1 is known to regulate the relative abundance of miRNAs (32) and some miRNAs have been reported to interfere with IAV replication, such as miR-584-5p and miR-1.249, or miR-323, miR-491 and miR-654, respectively inhibiting H5N1 and H1N1 by targeting PB2 and PB1 genes (60,61). ERI1 could therefore be recruited by the IAV vRNPs to target specific miRNA degradation and thus promote viral replication overall. Sequencing the miRNA repertoire upon ERI1 silencing would thus help addressing a potential role of ERI1 in miRNA homeostasis during IAV infection.

ERI1 targeting by IAV is thus another example supporting the growing evidence of the complex viral hijacking of cellular RNA decay machineries that rewires cellular gene expression in order to create a favorable environment for viral replication. Further work is needed to try and decipher the specific mechanisms, but the interaction identified between ERI1 and PB2/NP could already be considered as a potential target for the development of new antivirals.

DATA AVAILABILITY

The plasmid sequences were deposited into GenBank under accession numbers MT966965 to MT966999. All data and constructs are available upon request to sylvie.van-der-werf@pasteur.fr and caroline.demeret@pasteur.fr.

SUPPLEMENTARY DATA

Supplementary Data are available at NAR Online.

ACKNOWLEDGEMENTS

The authors would like to thank Patricia Cassonnet, Mélanie Dos Santos, Klea Riçku and Brian Townsend for help with experiments, Daniel Marc for the NS1 antibody as well as colleagues of the Unité Génétique Moléculaire des Virus à ARN and Florian Bakoa for helpful discussions.
Author contribution: Conceptualization: C.B., C.D., S.V.D.W.; Investigation: M.D., E.B., M.K., N.P.; Formal Analysis: M.D., E.B., N.P.; Visualization: M.D.; Funding acquisition: S.V.D.W.; Writing – Original Draft Preparation: M.D.; Writing – Review & Editing: M.D., C.B., C.D., S.V.D.W., Y.J.

FUNDING

European Union Seventh Framework Program (FP7/2007–2013) [278433-PREDEMICS: Preparedness, Prediction and Prevention of Emerging Zoonotic Viruses with Pandemic Potential using Multidisciplinary Approaches]; LabEx Integrative Biology of Emerging Infectious Diseases [10-LABX-0062]; Ministère de l'Education Nationale, de la Recherche et de Technologie [PhD fellowships from Université Paris Diderot/Université de Paris to M.D. and E.B.]; Fondation pour la Recherche Médicale [Programme Fin de thèse FDT201805005278 to M.D.]; Marie Skłodowska-Curie European Union Horizon 2020 research and innovation program [665850 to M.K.]. Funding for open access charge: Unité Génétique Moléculaire des Virus à ARN, UMR3569 CNRS, Université de Paris, Département de Virologie, Institut Pasteur, Paris, France.
Conflict of interest statement. None declared.

REFERENCES

1. Łabno,A., Tomecki,R. and Dziembowski,A. (2016) Cytoplasmic RNA decay pathways - enzymes and mechanisms. *Biochim. Biophys. Acta - Mol. Cell Res.*, **1863**, 3125–3147.
2. Mugridge,J.S., Coller,J. and Gross,J.D. (2018) Structural and molecular mechanisms for the control of eukaryotic 5′–3′ mRNA decay. *Nat. Struct. Mol. Biol.*, **25**, 1077–1085.
3. Gaglia,M.M. and Glaunsinger,B.A. (2010) Viruses and the cellular RNA decay machinery. *Wiley Interdiscip. Rev. RNA*, **1**, 47–59.
4. Molleston,J.M. and Cherry,S. (2017) Attacked from all Sides: RNA decay in antiviral defense. *Viruses*, **9**, 2.
5. Abernathy,E. and Glaunsinger,B. (2015) Emerging roles for RNA degradation in viral replication and antiviral defense. *Virology*, **479–480**, 600–608.
6. Balistreri,G., Bognanni,C., Mühlemann,O., Balistreri,G., Bognanni,C. and Mühlemann,O. (2017) Virus escape and manipulation of cellular nonsense-mediated mRNA decay. *Viruses*, **9**, 24.
7. Guo,L., Vlasova-St Louis,I. and Bohjanen,P.R. (2018) Viral manipulation of host mRNA decay. *Future Virol.*, **13**, 211–223.
8. Moon,S.L. and Wilusz,J. (2013) Cytoplasmic viruses: rage against the (cellular RNA decay) machine. *PLoS Pathog.*, **9**, e1003762.
9. Li,Y., Yamane,D. and Lemon,S.M. (2015) Dissecting the roles of the 5′ exoribonucleases Xrn1 and Xrn2 in restricting hepatitis C virus replication. *J. Virol.*, **89**, 4857–4865.
10. Kincaid,R.P., Lam,V.L., Chirayil,R.P., Randall,G. and Sullivan,C.S. (2018) RNA triphosphatase DUSP11 enables exonuclease XRN-mediated restriction of hepatitis C virus. *Proc. Natl. Acad. Sci. U.S.A.*, **115**, 8197–8202.
11. Molleston,J.M., Sabin,L.R., Moy,R.H., Menghani,S. V., Rausch,K., Gordesky-Gold,B., Hopkins,K.C., Zhou,R., Jensen,T.H., Wilusz,J.E. *et al.* (2016) A conserved virus-induced cytoplasmic TRAMP-like complex recruits the exosome to target viral RNA for degradation. *Genes Dev.*, **30**, 1658–1670.
12. Scheller,N., Mina,L.B., Galao,R.P., Chari,A., Gimenez-Barcons,M., Noueiry,A., Fischer,U., Meyerhans,A. and Diez,J. (2009) Translation and replication of hepatitis C virus genomic RNA depends on ancient cellular proteins that control mRNA fates. *Proc. Natl. Acad. Sci. U.S.A.*, **106**, 13517–13522.
13. Galão,R.P., Chari,A., Alves-Rodrigues,I., Lobão,D., Mas,A., Kambach,C., Fischer,U. and Díez,J. (2010) LSm1-7 complexes bind to specific sites in viral RNA genomes and regulate their translation and replication. *RNA*, **16**, 817–827.
14. Lee,C.-C., Lin,T.-L., Lin,J.-W., Han,Y.-T., Huang,Y.-T., Hsu,Y.-H. and Meng,M. (2016) Promotion of Bamboo Mosaic Virus Accumulation in Nicotiana benthamiana by 5′→3′ Exonuclease NbXRN4. *Front. Microbiol.*, **6**, 1508.
15. Ward,A.M., Calvert,M.E.K., Read,L.R., Kang,S., Levitt,B.E., Dimopoulos,G., Bradrick,S.S., Gunaratne,J. and

Garcia-Blanco,M.A. (2016) The Golgi associated ERI3 is a Flavivirus host factor. *Sci. Rep.*, **6**, 34379.
16. Pijlman,G.P., Funk,A., Kondratieva,N., Leung,J., Torres,S., van der Aa,L., Liu,W.J., Palmenberg,A.C., Shi,P.-Y., Hall,R.A. *et al.* (2008) A highly structured, Nuclease-Resistant, noncoding RNA produced by flaviviruses is required for pathogenicity. *Cell Host Microbe*, **4**, 579–591.
17. Shaw,M.L. and Stertz,S. (2017) In: *Role of Host Genes in Influenza Virus Replication*. Springer, Cham, pp. 151–189.
18. Peacock,T.P., Sheppard,C.M., Staller,E. and Barclay,W.S. (2019) Host determinants of influenza RNA synthesis. *Annu. Rev. Virol.*, **6**, 215–233.
19. Krammer,F., Smith,G.J.D., Fouchier,R.A.M., Peiris,M., Kedzierska,K., Doherty,P.C., Palese,P., Shaw,M.L., Treanor,J., Webster,R.G. *et al.* (2018) Influenza. *Nat. Rev. Dis. Prim.*, **4**, 3.
20. te Velthuis,A.J.W. and Fodor,E. (2016) Influenza virus RNA polymerase: insights into the mechanisms of viral RNA synthesis. *Nat. Rev. Microbiol.*, **14**, 479–493.
21. De Vlugt,C., Sikora,D., Pelchat,M., De Vlugt,C., Sikora,D. and Pelchat,M. (2018) Insight into influenza: a virus cap-snatching. *Viruses*, **10**, 641.
22. Min,J.-Y., Li,S., Sen,G.C. and Krug,R.M. (2007) A site on the influenza A virus NS1 protein mediates both inhibition of PKR activation and temporal regulation of viral RNA synthesis. *Virology*, **363**, 236–243.
23. Paterson,D. and Fodor,E. (2012) Emerging roles for the influenza A virus nuclear export protein (NEP). *PLoS Pathog.*, **8**, e1003019.
24. Martin,K. and Heleniust,A. (1991) Nuclear transport of influenza virus ribonucleoproteins: The viral matrix protein (M1) promotes export and inhibits import. *Cell*, **67**, 117–130.
25. Qu,H., Li,J., Yang,L., Sun,L., Liu,W. and He,H. (2016) Influenza A virus-induced expression of ISG20 inhibits viral replication by interacting with nucleoprotein. *Virus Genes*, **52**, 759–767.
26. Min,J.-Y. and Krug,R.M. (2006) The primary function of RNA binding by the influenza A virus NS1 protein in infected cells: Inhibiting the 2′-5′ oligo (A) synthetase/RNase L pathway. *Proc. Natl. Acad. Sci. U.S.A.*, **103**, 7100–7105.
27. Khaperskyy,D.A., Schmaling,S., Larkins-Ford,J., McCormick,C. and Gaglia,M.M. (2016) Selective degradation of host RNA polymerase II transcripts by influenza A virus PA-X host shutoff protein. *PLoS Pathog.*, **12**, e1005427.
28. Rialdi,A., Hultquist,J., Jimenez-Morales,D., Peralta,Z., Campisi,L., Fenouil,R., Moshkina,N., Wang,Z.Z., Laffleur,B., Kaake,R.M. *et al.* (2017) The RNA exosome syncs IAV-RNAPII transcription to promote viral ribogenesis and infectivity. *Cell*, **169**, 679–692.
29. Tan,D., Marzluff,W.F., Dominski,Z. and Tong,L. (2013) Structure of histone mRNA stem-loop, human stem-loop binding protein and 3′hExo ternary complex. *Science*, **339**, 318.
30. Yang,X.C., Purdy,M., Marzluff,W.F. and Dominski,Z. (2006) Characterization of 3′hExo, a 3′ exonuclease specifically interacting with the 3′ end of histone mRNA. *J. Biol. Chem.*, **281**, 30447–30454.
31. Cheng,Y. and Patel,D.J. (2004) Crystallographic structure of the nuclease domain of 3′hExo, a DEDDh family member, bound to rAMP. *J. Mol. Biol.*, **343**, 305–312.
32. Thomas,M.F., Abdul-Wajid,S., Panduro,M., Babiarz,J.E., Rajaram,M., Woodruff,P., Lanier,L.L., Heissmeyer,V., Ansel,K.M., Brusco,A. *et al.* (2012) Eri1 regulates microRNA homeostasis and mouse lymphocyte development and antiviral function. *Blood*, **120**, 130–142.
33. Ansel,K.M., Pastor,W.A., Rath,N., Lapan,A.D., Glasmacher,E., Wolf,C., Smith,L.C., Papadopoulou,N., Lamperti,E.D., Tahiliani,M. *et al.* (2008) Mouse Eri1 interacts with the ribosome and catalyzes 5.8S rRNA processing. *Nat. Struct. Mol. Biol.*, **15**, 523–530.
34. Gabel,H.W. and Ruvkun,G. (2008) The exonuclease ERI-1 has a conserved dual role in 5.8S rRNA processing and RNAi. *Nat. Struct. Mol. Biol.*, **15**, 531–533.
35. Hoefig,K.P., Rath,N., Heinz,G.A., Wolf,C., Dameris,J., Schepers,A., Kremmer,E., Ansel,K.M. and Heissmeyer,V. (2013) Eri1 degrades the stem-loop of oligouridylated histone mRNAs to induce replication-dependent decay. *Nat. Struct. Mol. Biol.*, **20**, 73–81.
36. Thomas,M.F., L'Etoile,N.D. and Ansel,K.M. (2014) Eri1: a conserved enzyme at the crossroads of multiple RNA-processing pathways Elsevier Current Trends. *Trends Genet.*, **30**, 298–307.
37. Matrosovich,M., Matrosovich,T., Carr,J., Roberts,N.A. and Klenk,H.-D. (2003) Overexpression of the alpha-2, 6-sialyltransferase in MDCK cells increases influenza virus sensitivity to neuraminidase inhibitors. *J. Virol.*, **77**, 8418–8425.
38. Biquand,E., Poirson,J., Karim,M., Declercq,M., Malausse,N., Cassonnet,P., Barbezange,C., Straub,M., Jones,L., Munier,S. *et al.* (2017) Comparative profiling of ubiquitin proteasome system interplay with influenza A virus PB2 polymerase humans. *mSphere*, **2**, e00330-17.
39. Cassonnet,P., Rolloy,C., Neveu,G., Vidalain,P.-O., Chantier,T., Pellet,J., Jones,L., Muller,M., Demeret,C., Gaud,G. *et al.* (2011) Benchmarking a luciferase complementation assay for detecting protein complexes. *Nat. Methods*, **8**, 990–992.
40. Bindea,G., Mlecnik,B., Hackl,H., Charoentong,P., Tosolini,M., Kirilovsky,A., Fridman,W.-H., Pagès,F., Trajanoski,Z. and Galon,J. (2009) ClueGO: a Cytoscape plug-in to decipher functionally grouped gene ontology and pathway annotation networks. *Bioinformatics*, **25**, 1091–1093.
41. Kanehisa,M. and Goto,S. (2000) KEGG: kyoto encyclopedia of genes and genomes. *Nucleic Acids Res.*, **28**, 27–30.
42. Alonso-López,D., Gutiérrez,M.A., Lopes,K.P., Prieto,C., Santamaría,R. and De Las Rivas,J. (2016) APID interactomes: providing proteome-based interactomes with controlled quality for multiple species and derived networks. *Nucleic Acids Res.*, **44**, W529–W535.
43. Tafforeau,L., Chantier,T., Pradezynski,F., Pellet,J., Mangeot,P.E., Vidalain,P.-O., Andre,P., Rabourdin-Combe,C. and Lotteau,V. (2011) Generation and comprehensive analysis of an influenza virus polymerase cellular interaction network. *J. Virol.*, **85**, 13010–13018.
44. Munier,S., Rolland,T., Diot,C., Jacob,Y. and Naffakh,N. (2013) Exploration of binary virus-host interactions using an infectious protein complementation assay. *Mol. Cell. Proteomics*, **12**, 2845–2855.
45. Matrosovich,M., Matrosovich,T., Garten,W. and Klenk,H.-D. (2006) New low-viscosity overlay medium for viral plaque assays. *Virol. J.*, **3**, 63.
46. Vignuzzi,M., Gerbaud,S., van der Werf,S. and Escriou,N. (2001) Naked RNA immunization with replicons derived from poliovirus and Semliki Forest virus genomes for the generation of a cytotoxic T cell response against the influenza A virus nucleoprotein. *J. Gen. Virol.*, **82**, 1737–1747.
47. Kawakami,E., Watanabe,T., Fujii,K., Goto,H., Watanabe,S., Noda,T. and Kawaoka,Y. (2011) Strand-specific real-time RT-PCR for distinguishing influenza vRNA, cRNA, and mRNA. *J. Virol. Methods*, **173**, 1–6.
48. Brodersen,M.M.L., Lampert,F., Barnes,C.A., Soste,M., Piwko,W. and Peter,M. (2016) CRL4 WDR23 -Mediated SLBP ubiquitylation ensures histone supply during DNA replication. *Mol. Cell*, **62**, 627–635.
49. Marzluff,W.F. and Koreski,K.P. (2017) Birth and death of histone mRNAs. *Trends Genet.*, **33**, 745–759.
50. Mok,B.W.-Y., Song,W., Wang,P., Tai,H., Chen,Y., Zheng,M., Wen,X., Lau,S.-Y., Wu,W.L., Matsumoto,K. *et al.* (2012) The NS1 protein of influenza A virus interacts with cellular processing bodies and stress granules through RNA-Associated protein 55 (RAP55) during virus infection. *J. Virol.*, **86**, 12695–12707.
51. Bauer,D.L. V, Tellier,M., Martínez-Alonso,M., Nojima,T., Proudfoot,N.J., Murphy,S. and Fodor,E. (2018) Influenza virus mounts a two-pronged attack on host RNA polymerase II transcription. *Cell Rep.*, **23**, 2119–2129.
52. de Chassey,B., Aublin-Gex,A., Ruggieri,A., Meyniel-Schicklin,L., Pradezynski,F., Davoust,N., Chantier,T., Tafforeau,L., Mangeot,P.-E., Ciancia,C. *et al.* (2013) The interactomes of influenza virus NS1 and NS2 proteins identify new host factors and provide insights for ADAR1 playing a supportive role in virus replication. *PLoS Pathog.*, **9**, e1003440.
53. Han,J., Perez,J.T., Chen,C., Li,Y., Benitez,A., Kandasamy,M., Lee,Y., Andrade,J., tenOever,B. and Manicassamy,B. (2018) Genome-wide CRISPR/Cas9 screen identifies host factors essential for influenza virus replication. *Cell Rep.*, **23**, 596–607.
54. Wu,K.X., Phuektes,P., Kumar,P., Goh,G.Y.L., Moreau,D., Chow,V.T.K., Bard,F. and Chu,J.J.H. (2016) Human genome-wide RNAi screen reveals host factors required for enterovirus 71 replication. *Nat. Commun.*, **7**, 13150.

55. Silva-Ayala,D., Lopez,T., Gutierrez,M., Perrimon,N., Lopez,S. and Arias,C.F. (2013) Genome-wide RNAi screen reveals a role for the ESCRT complex in rotavirus cell entry. *Proc. Natl. Acad. Sci. U.S.A.*, **110**, 10270–10275.
56. Lee,A.S.-Y., Burdeinick-Kerr,R. and Whelan,S.P.J. (2014) A Genome-Wide small interfering RNA screen identifies host factors required for vesicular stomatitis virus infection. *J. Virol.*, **88**, 8355.
57. Khaperskyy,D.A., Schmaling,S., Larkins-Ford,J., McCormick,C. and Gaglia,M.M. (2016) Selective degradation of host RNA polymerase II transcripts by influenza A virus PA-X host shutoff protein. *PLOS Pathog.*, **12**, e1005427.
58. Eckerle,L.D., Becker,M.M., Halpin,R.A., Li,K., Venter,E., Lu,X., Scherbakova,S., Graham,R.L., Baric,R.S., Stockwell,T.B. *et al.* (2010) Infidelity of SARS-CoV Nsp14-exonuclease mutant virus replication is revealed by complete genome sequencing. *PLoS Pathog.*, **6**, e1000896.
59. Hastie,K.M., Kimberlin,C.R., Zandonatti,M.A., MacRae,I.J. and Saphire,E.O. (2011) Structure of the Lassa virus nucleoprotein reveals a dsRNA-specific 3′ to 5′ exonuclease activity essential for immune suppression. *Proc. Natl. Acad. Sci. U.S.A.*, **108**, 2396–2401.
60. Wang,R., Zhang,Y.-Y., Lu,J.-S., Xia,B.-H., Yang,Z.-X., Zhu,X.-D., Zhou,X.-W. and Huang,P.-T. (2017) The highly pathogenic H5N1 influenza A virus down-regulated several cellular MicroRNAs which target viral genome. *J. Cell. Mol. Med.*, **21**, 3076–3086.
61. Song,L., Liu,H., Gao,S., Jiang,W. and Huang,W. (2010) Cellular microRNAs inhibit replication of the H1N1 influenza A virus in infected cells. *J. Virol.*, **84**, 8849–8860.